ISSN 0040-5795, Theoretical Foundations of Chemical Engineering, 2015, Vol. 49, No. 6, pp. 869–876. © Pleiades Publishing, Ltd., 2015.

Determination of Metastable Zone Width and the Primary Nucleation Kinetics of Sodium Sulfate[1]

Guisheng Zeng[a, b, *], Hui Li[a], Sheng Huang[a], Xianyong Wang[a], and Junhong Chen[b]

[a] *Key Laboratory of Jiangxi Province for Persistent Pollutants Control and Resources Recycle, School of Environment and Chemical Engineering, Nanchang Hangkong University, Nanchang 330063, China*

[b] *Department of Mechanical Engineering, University of Wisconsin-Milwaukee, Milwaukee, Wisconsin 53211, United States*

e-mail: zengguisheng@hotmail.com

Received February 25, 2013

Abstract—The saturation curve, metastable zone width (MSZW) and primary nucleation kinetics were measured and estimated during sodium sulfate cooling crystallization process. The MSZW is commonly used to characterize crystal nucleation and determine the operation window for crystallization process. The MSZW is the difference between the saturation temperature and the temperature at which crystals are formed at different temperatures, cooling rates and agitating rates. The approach to interpret the MSZW obtained by polythermal method using the classical nucleation theory by Nyvlt was extended. Interfacial energy was determined for the growth of sodium sulfate crystals. Nucleation parameters such as surface entropy factor, radius of critical nucleus, Gibbs free energy, and critical energy barrier were investigated. The nucleation order was established based on the measurements of MSZW dependence on cooling rate and agitating rate. It was experimentally observed that there is rise of solubility with increase of temperature. When the temperature becomes higher, solubility gradually declines. In this investigation, MSZW was observed to enhance with increase of cooling rate and decrease with increase of agitating rate.

Keywords: sodium sulfate, metastable zone width, crystallization, thermodynamics

DOI: 10.1134/S0040579515050309

INTRODUCTION

Crystallization is adopted in separation and purification process in pharmaceutical, food, fine chemical and material industries [1–4]. It is a very important unit operation involves the separation of solid phase from its original liquid phase system. Industrially it accounts for over 70% of solids produced in the chemical process and pharmaceutical industries. Especially, MSMPR crystallizer is widely used and laboratorial researches benefited to perform crystallization of industrial standard. According to the method in laboratory research, industrial crystallization may choose suited crystallizer to produce the crystal products. The crystal products must have not only high purity and high yield but also rationality of crystal size and size distribution in industrial crystallization. To achieve such a goal, crystallization thermodynamics such as solubility and metastable zone width (MSZW) are investigated. MSZW measurements have become an operation platform to characterize nucleation and to evaluate the crystallization process. The creation of new solid interfaces required a certain level of supersaturation that is also known as super-solubility. The region between super-solubility and solubility curve is known as MSZW, as shown in Fig. 1. Investigation of solubility and MSZW of solutions has become an active research field for over four decades. MSZW is determined experimentally by the various methods in which the detection of "first crystals" is monitored when the solution is continuously cooled at a constant rate. Due to its significance in nucleation and crystal growth, MSZW is considered as an important param-

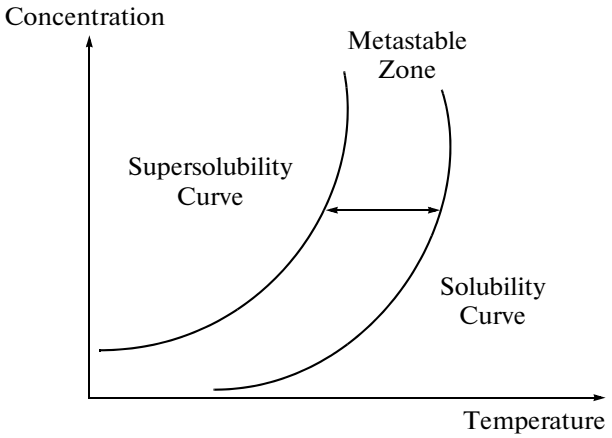

Fig. 1. Solubility curve and MSZW.

[1] The article is published in the original.

eter in the specification of products obtained from industrial crystallization process. K. Selvaraju studied the MSZW of non-linear optical L-Glutamic Acid Hydrochloride single crystals [5]. Kwang-Joo Kim estimated the MSZW in different nucleation processes [6]. Sibel Titiz-Sargut determined the MSZW under three cooling rates by means of an ultrasonic measuring technique [7]. M. Trifkovic measured the MSZW, induction time and primary nucleation kinetics for anti-solvent and cooling crystallization [8]. MSZW measured can be affected by numerous process parameters, such as cooling rate [9], agitation rate [10], presence of impurity [11], solution [12], supersaturation ratio [13] and working volume [14], etc.

Sodium sulfate is used in a large scale in glass, synthetic fiber, paper and other industries. The demand of sodium sulfate crystal in different particle sizes is always a problem for manufacturers. In order to develop crystallization process to meet the desired ends, crystallization thermodynamics including solubility, crystal size distribution (CSD) and MSZW are investigated. For example, theoretical and experimental investigation were conducted by Azimi to study the solubility of gypsum and anhydrite in simulated laterite pressure acid leach (PAL) solutions in the temperature range of 25–250°C [15]. Also, Marliacy obtained the crystallization thermodynamics of sodium sulfate decahydrate in H_2O–NaCl–Na_2SO_4 [16]. In natural, heterogeneous (non-equilibrium) systems, heterogeneous nucleation of sodium sulfate are promoted at temperatures below 32.4°C at low RH, fast solution evaporation, and high supersaturation ratios [17]. The phase diagram of Na_2SO_4–H_2O system was updated based on a careful review of the available thermodynamic data of aqueous sodium sulfate and the crystalline phases [18]. The climatic conditions (temperature and evaporation rate) have an influence on the sodium sulfate phase crystallizing and the concentration of the solution at the point of crystallization [19]. Nonetheless, reports on theoretical studies of MSZW, primary nucleation kinetics, nucleation parameters such as surface entropy factor, radius of critical nucleus, Gibbs free energy, and critical energy barrier are few.

In this paper, a 100 mL double jacketed glass crystallizer was used to imitate MSMPR crystallizer. The solubility curve of sodium sulfate as well as the effect of cooling rate and agitating rate on MSZW was reported. The experimental MSZW data measured in this work was employed to estimate the nucleation kinetics of sodium sulfate. Besides, nucleation order and parameters were obtained based on the classical nucleation theory.

EXPERIMENTAL DETAILS

Solubility measurement. The solubility was determined through a balance method by using a laboratory-designed constant temperature water cycle system similar to those reported in the literature [20]. The samples were weighed using an analytical balance (Sartorious CP224S, Germany) with an uncertainty of ±0.0001 g. Excess amount of sodium sulfate (M_1) were dissolved stirringly in 100 mL distilled water in the jacketed glass crystallizer. The stirring process must last for at least 12 h to make sure that the dissolve reaction reached balance. After achieving the equilibrium, the remaining sodium sulfate were separated by suction filtration dried and weighed (M_2). Solubility of sodium sulfate can be achieved by calculating the gravimetric differential and expresses as follows:

$$S = \frac{\text{solute}}{\text{solution}} \times 100\% = (M_1 - M_2) \times 100\%.$$

All of the measurements were repeated at least three times, and the average of the measurements is considered to be the solubility. Using the same method, the solubility of sodium sulfate at a number of designated temperatures was obtained.

MSZW measurement. Super-solubility curve. Firstly, the saturated solution of sodium sulfate was prepared in a beaker using an approach similar to that adopted for the determination of solubility data described above. The solution in jacketed glass crystallizer was maintained at a constant temperature by constant-temperature control system (GDH-3006, Ningbo Xinzhi Co., Ltd., China). Then the solution was heated 5 degrees above the saturation temperature for homogenization and was kept at the superheated temperature for about one hour. When the system begins cooling, a self-design laser detection system was used to detect crystal nucleus and thermometer was used to record temperature. The temperature when first nucleation was detected visually was recorded. A self-design experimental apparatus is similar to many other researchers' [20–21]. The supersolubility curve was drawn based on the experimental data. The distance between solubility curve and supersolubility curve is the MSZW.

Effect of cooling rate and agitating rate on MSZW. The effect of cooling rate on MSZW was investigated based on the phenomena observed at three different cooling rates (8°C/min, 11°C/min, and 14°C/min). Then with the saturated solution kept at a constant temperature and adopting a constant cooling rate. The effect of agitating rate on MSZW was also studied based on the phenomena observed at three different agitating rates (300, 600, 900 rpm). The mechanical agitator (EUROSTAR 20 digital, IKA, Germany) was used in experiments.

Primary nucleation kinetics. Nucleation order. With adequate MSZW data, it is possible to conduct research on the nucleation kinetics of sodium sulfate. Classical nucleation theory can be applied to the MSZW data collected at different cooling rates and agitating rates. The approach for the estimation of nucleation kinetics from MSZW results is based on the work of Nyvlt [22]. It can be shown that utilizing clas-

sical nucleation theory, the nucleation rate can be expressed as

$$J = \frac{dN}{dt} = k_0'\Delta c^n, \quad (1)$$

where k_0' is the nucleation rate constant, Δc is the supersaturation ($\Delta c = c - c^*$), n is the cooling rate. During cooling crystallization, the rate of supersaturation generation can be expressed as a function of the cooling rate n, as follows:

$$\frac{d\Delta c}{dt} = n - \frac{dc^*}{dT}. \quad (2)$$

At the point of nucleation, the supersaturation is related to MSZW by

$$\Delta c_{\max} = \Delta T_{\max}\frac{dc^*}{dT}, \quad (3)$$

where MSZW is given by

$$\Delta T_{\max} = T^* - T_{\text{nuc}}. \quad (4)$$

At the point of nucleation, it may be assumed that the rate of supersaturation generation equals the rate of formation of new crystals which is given by [22]

$$\frac{dM}{dt} = k_n\alpha\rho_c n^3\Delta c^{m'} = k_n\Delta c^{m'}. \quad (5)$$

Combining equations (2), (3) and (5), one obtains

$$\ln n = (m' - 1)\ln\left(\frac{dc^*}{dT}\right) + \ln(k_n) + m'\ln(\Delta T_{\max}). \quad (6)$$

According to the above equation, a plot of $\ln n$ versus $\ln(\Delta T_{\max})$ for a given saturation temperature should result in a straight line, with the slope yielding the apparent nucleation order m', and the mass nucleation rate constant, k_n, estimated from y-intercept.

Nucleation parameter. The original data of induction period were taken from the experimental results of Chen Xia [23] that is related to the relationship between induction period and supersaturation ratio during cooling crystallization.

A driving force is taken from the change of Gibbs free energy (ΔG) between the surrounding parent solution and the crystalline phase that stimulates crystallization. The energy needed for the generation of sodium sulfate nuclei is given by equation (7) [24].

$$\Delta G = 4/3\pi r^3\Delta G_v + 4\pi r^2\gamma, \quad (7)$$

where ΔG_v is the energy change per unit volume, γ the interfacial tension, r the radius of nucleus. The free energy formation obeys the condition $d(\Delta G)/dr = 0$ at the critical state. Hence the radius of critical nucleus is expressed as equation (8)

$$r^* = \frac{-2\gamma}{\Delta G_v}, \quad (8)$$

where $\Delta G_v = -\Delta\mu/v$, $\Delta\mu = -kT\ln S$, here $S = C/C^*$, v is the molar volume of the crystal, T temperature of the solution in K, k the Boltzmann's constant, S the supersaturation ratio, C the actual concentration of the solution, and C^* the equilibrium concentration of the solution. Hence, the radius of critical nucleus r^* can be expressed as

$$r^* = \frac{-2v\gamma}{\Delta\mu}. \quad (9)$$

The critical free energy barrier is

$$\Delta G^* = \frac{16\pi\gamma^3 v^3}{3\Delta\mu^2}. \quad (10)$$

The interfacial tension is a critical parameter involved in between a growing crystal and the surrounding parent liquor. In the current investigation, interfacial tension was computed based on the experimentally determined induction period values using the following relation on the basis of classical nucleation theory for homogeneous formation of spherical nuclei, the relationship between induction time and supersatluration can expressed as follows:

$$\ln t_{\text{ind}} = K + \frac{16\pi\gamma^3 V_m}{3v^2k^3T^3\ln^2 S}, \quad (11)$$

where v is the molar volume of the crystals, S the supersaturation ratio, and t_{ind} the induction period of sodium sulfate solution at temperature T. K is a constant. A plot of $1/(\ln S)^2$ against $\ln t_{\text{ind}}$ is a straight line. The y-intercept of the straight line gives the value of const.

The equation explains a linear fit for $\ln t_{\text{ind}}$ against $1/(\ln S)^2$ with a slope given by

$$m = \frac{16\pi\gamma^3 v^2}{3k^3T^3}. \quad (12)$$

The interfacial tension can be expressed as

$$\gamma = \left(\frac{3mk^3T^3}{16\pi v^2}\right)^{\frac{1}{3}}, \quad (13)$$

where m is the slope of the straight line.

Surface entropy factor f can be described as

$$f = \frac{4\upsilon^{2/3}\gamma}{kT}. \quad (14)$$

RESULTS AND DISCUSSIONS

Metasatable zone width. Figure 2 shows the solubility and super-solubility of sodium sulfate at different temperature. It can be seen that the solubility of sodium sulfate has an inflection point at 34°C. The change is due to the existence of crystals of different forms close to the inflection point. There is an increase of solubility with temperature rise. When the temperature is higher than that of the inflection point, the solubility curve shows a slow downward trend. Below 34°C, Glauber salt ($Na_2SO_4 \cdot 10H_2O$) is separated out from the supersaturated solution. There is heat absorption during the dissolution of Glauber salt. According to thermal equilibrium, the heat is more likely to move to the endothermic direction with increasing temperature. Thus, with increase of tem-

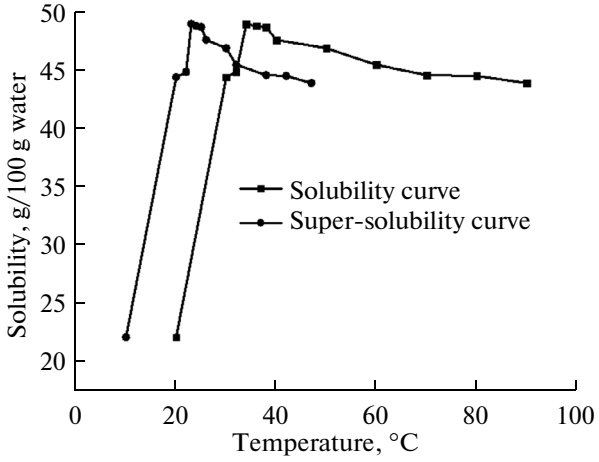

Fig. 2. The graph of solubility and super-solubility curve.

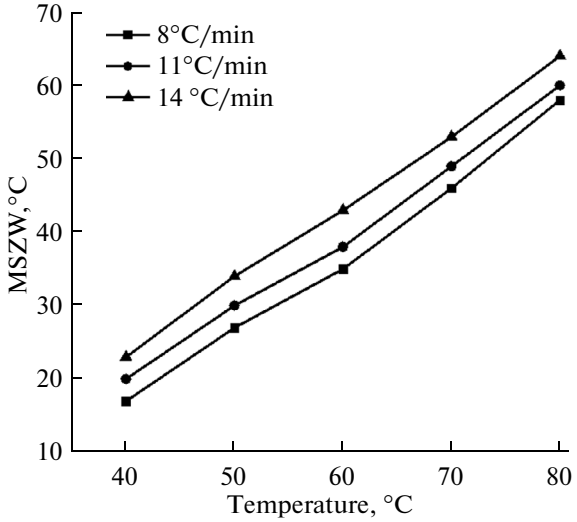

Fig. 3. The effect of cooling rate on the MSZW.

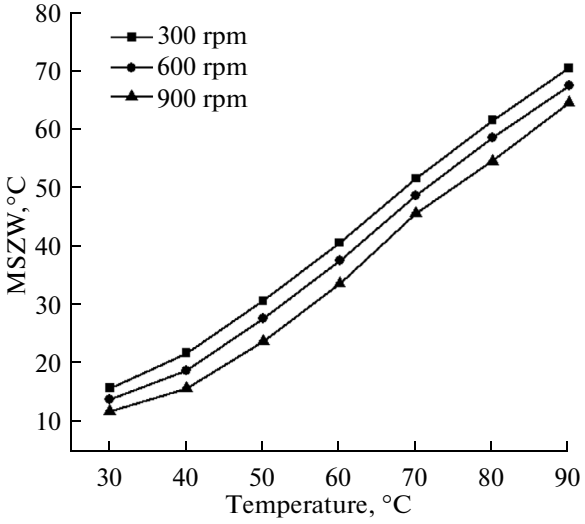

Fig. 4. The effect of agitating rate on the MSZW.

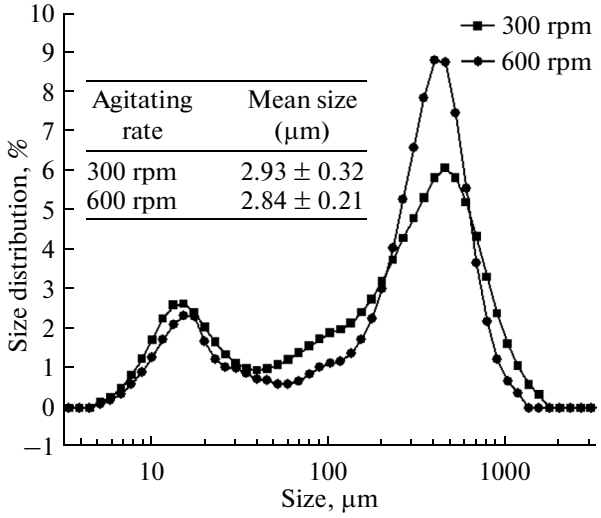

Fig. 5. The CSD of sodium sulfate under different agitating rate.

perature, there is an increase of sodium sulfate concentration. When the temperature is above 34°C, the dissolution of sodium sulfate crystal becomes exothermic. Thus with temperature rise, there is a decline in the concentration of sodium sulfate. The MSZW slightly enlarges with the increase of temperature as shown in Fig. 2. It is obvious that there is a decrease in collision of solute molecules and nucleation rate when in higher temperature. And when decrease of solubility with temperature rise, the MSZW enlargement.

Figure 3 shows the effect of cooling rate on MSZW. With increase of cooling rate, there is a clear trend of MSZW widening. At constant temperature, the increase of cooling rate makes nucleation process easier. The experimental data are qualitatively in good agreement with the curve of heterogeneous nucleation. Figure 4 shows the influence of agitating rate on MSZW. The MSZW dramatically decreases with increasing agitating rate at a particular cooling rate. Mass transfer rate and molecule collision, nucleation rate increases with increase of agitating rate. At the same time, there is increase of heat transfer rate that is beneficial for heat diffusion and supersaturation reduction. The CSD of sodium sulfate under different agitating rate was determined by Malvin laser particle size analyzer. The results were shown in Fig. 5. From Fig. 5, an obvious phenomenon was found with two peaks of sodium sulfate, which has not been reported at the history of sodium sulfate according to the literature reported before. The first peak may be represented the stage of nuclei generating, and the second stage indicated the formation of crystals. The mean

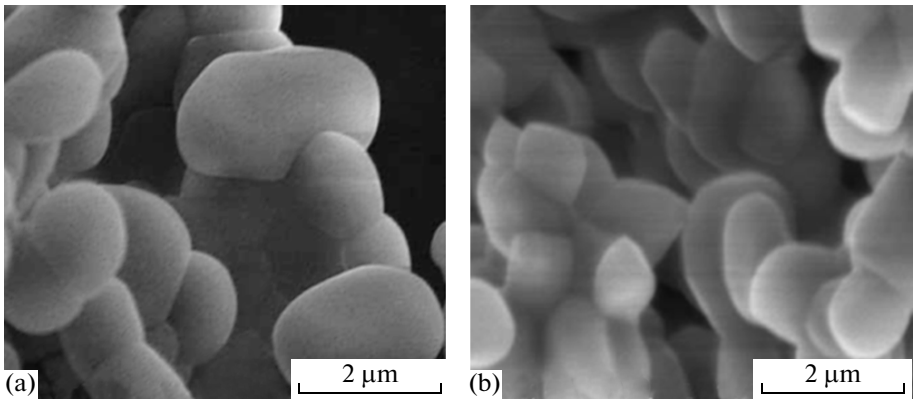

Fig. 6. The SEM of sodium sulfate crystals under different cooling rate (a) 8°C/min, (b) 14°C/min.

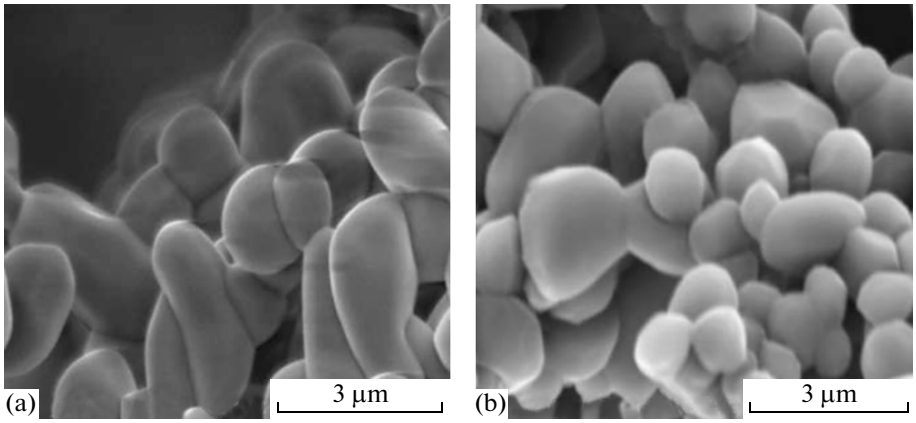

Fig. 7. The SEM of sodium sulfate crystals under different cooling rate and agitating rate (a) 300 (b) 900 rpm.

size of crystals decreases from 2.93 ± 0.32 to 2.84 ± 0.21 μm, as the stirring rate increases from 300 to 600 rpm. When the stir rate increases, nucleation rate increased and growth rate decreased which lead to the decrease of mean size.

It can be seen that the average size decreases with the increase of cooling and agitating rate from Fig. 6 and 7. With the increase of agitating rate, the agglomeration phenomenon was obviously reduced because of broken of crystals from Fig. 7. But the cooling and agitating rate have no influence on the crystal shape which is spherical.

Primary kinetics. Nucleation order. The relationship of $\ln b$ and $\ln(\Delta T_{max})$ is shown in Fig. 8. Using equation (6), the nucleation orders can be readily obtained from the MSZW data. As shown in Fig. 8, the nucleation orders appear to be a function of cooling rate. Table 1 shows the calculated nucleation equation and orders for sodium sulfate. The nucleation order ranges from 2.0765 to 6.1741, which is in good agree-

Table 1. Nucleation equation and orders under different cooling rates

Temperature, °C	Nucleation equation	Nucleation order $m'_{(b)}$
40	$\ln b = -3.8097 + 2.07651\ln(\Delta T_{max})$	2.0765
50	$\ln b = -6.8695 + 2.71871\ln(\Delta T_{max})$	2.7187
60	$\ln b = -8.5968 + 3.0104\ln(\Delta T_{max})$	3.0104
70	$\ln b = -14.8497 + 4.4176\ln(\Delta T_{max})$	4.4176
80	$\ln b = -22.9458 + 6.1741\ln(\Delta T_{max})$	6.1741

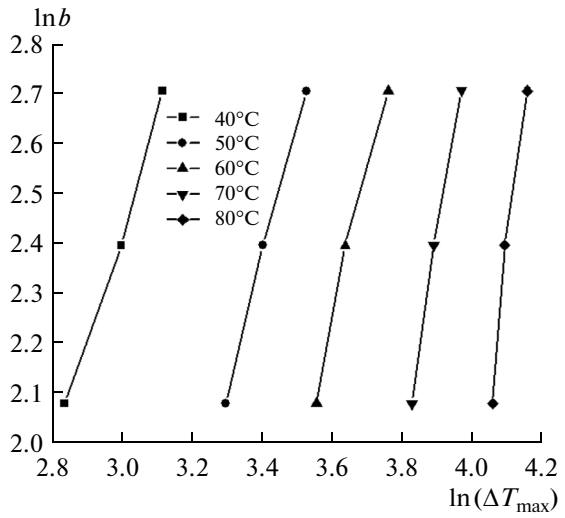

Fig. 8. The relationship of ln$b$ and ln(ΔT_{max}).

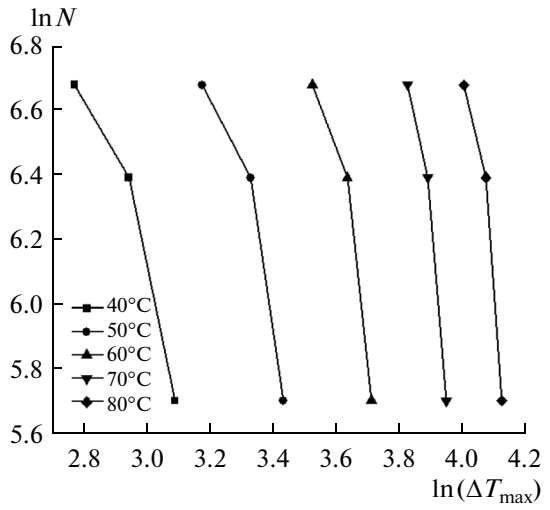

Fig. 9. The relationship of ln$N$ and ln(ΔT_{max}).

ment with that of the classic nucleation theory. It indicates that there is increase of nucleation order with rise of temperature and crystallization becomes more favorable when there is a decline in nucleation order. In solution, the density of activity solute molecule is low, they have less chance to gather together and nucleate, when stir was introduced part of solute molecule get across energy barrier then formed into crystal nucleus and high stir. The intermolecular collisions are more intensely with increasing of cooling rate. Thus, nucleus crystals are promoting obviously and nucleation rate is acceleratly to raise the nucleation order.

The relationship of ln$N$ and ln(ΔT_{max}) is shown in Fig. 9. Table 2 shows the calculated nucleation equation and orders for sodium sulfate under different agitating rate. Nucleation orders are Irregular changes from 0.6830 to 0.7800.

Thermodynamic parameters. From equation (11), the curve of lnt_{ind} vs. ln$S$ can be obtained ($m = 0.2272$) according to the literature. Interfacial tension value is a basic physical quantity of crystal nucleation and crystal growth. Using equation (13), one can obtain the interfacial tension ($\gamma = 3.2 \times 10^{-3}$ N m^{-1}). The nucleation parameters: Gibbs free energy per unit volume (ΔG_V), critical radius nucleus (r^*) and critical energy barrier (ΔG^*) of the growth of sodium sulfate crystals under various supersaturation conditions were shown in Table 3. Surface entropy factor ($f = 0.49$) can be attained from equation (14). When surface entropy factor is less than 3, the crystal growth fits well into the continuous growth model.

Table 2. Nucleation equation and orders under different agitating rates

Temperature, °C	Nucleation equation	Nucleation order $m'_{(N)}$
40	$\ln N = 15.1886 - 3.0405 \ln(\Delta T_{max})$	0.6830
50	$\ln N = 18.4391 - 3.6737 \ln(\Delta T_{max})$	0.7400
60	$\ln N = 24.5511 - 5.0441 \ln(\Delta T_{max})$	0.6544
70	$\ln N = 37.2432 - 7.96331 \ln(\Delta T_{max})$	0.5547
80	$\ln N = 38.4809 - 7.9150 \ln(\Delta T_{max})$	0.7800

Table 3. Nucleation parameters of sodium sulfate

S	ΔG_V	r^*	ΔG^*
0.5	-1.81×10^7	3.54×10^{-10}	0.32×10^{-48}
0.7	-0.93×10^7	6.90×10^{-10}	1.12×10^{-48}
0.9	-0.28×10^7	23.3×10^{-10}	14.00×10^{-48}

CONCLUSIONS

An optical and constant-temperature control system was designed and prepared for in situ observation of sodium sulfate cooling crystallization process. The solubility of sodium sulfate was determined and there shows an increase of solubility with the increasing of temperature. When the temperature is higher than that of the inflection point (34°C), the solubility curve shows a slow downward trend. The Metastable Zone Width (MSZW) became wider with the increases of temperature and cooling rate. There is dramatic decline of MSZW with increase of agitating rate at a constant temperature and at a certain cooling rate. The mean size of sodium sulfate decreases with the increase of cooling and agitating rate and the spherical shape of sodium sulfate crystals have not changed under different cooling and agitating rate. Nucleation orders were obtained in various cooling and agitating rate, respectively. Using classical nucleation theory, nucleation parameters such as interfacial tension, interfacial energy, and radius of critical nucleus, Gibbs free energy, and critical energy barrier were investigated. With increasing of temperature, there is an upward tendency in nucleation order. The obtained sodium sulfate CSD shows good quality for industrial crystallization. The present work already shows the potential to improve the control of sodium sulfate cooling crystallization process.

ACKNOWLEDGMENTS

This work was financially supported by the National Natural Science Foundation of China (51266011), the National High Technology Research and Development Program of China (2010AA065204), and the Jiangxi Provincial Department of Education (GJJ13505). We thank Prof. C. T. Au of the Hong Kong Baptist University (Adjunct professor of NCHKU) for helpful advices.

REFERENCES

1. Braatz, R.D., Advanced control of crystallization processes, *Annu. Rev. Control*, 2002, vol. 26, pp. 87–89.
2. Wohlgemuth, K., Kordylla, A., Ruether, F., and Schembecker, G., Experimental study of the effect of bubbles on nucleation during batch cooling crystallization, *Chem. Eng. Sci.*, 2009, vol. 64, pp. 4155–4163.
3. Lubelli, B. and Rooij, M.R., NaCl crystallization in restoration plasters, *Constr. Build. Mater.*, 2009, vol. 23, pp. 1736–1742.
4. Lorenzo, M.L. and Silvestre, C., Non-isothermal crystallization of polymers, *Prog. Polym. Sci.*, 1999, vol. 24, pp. 917–950.
5. Selvaraju, K., Valluvan, R., and Kumararaman, S., Experimental determination of metastable zone width, induction period, interfacial energy and growth of nonlinear optical l-glutamic acid hydrochloride single crystals, *Mater. Lett.*, 2006, vol. 60, pp. 1565–1569.
6. Kwang-Joo, K., and Alfons, M., Estimation of metastable zone width in different nucleation processes, *Chem. Eng. Sci.*, 2001, vol. 56, pp. 2315–2324.
7. Titiz-Sargut, S. and Ulrich, J., Application of a protected ultrasound sensor for the determination of the width of the metastable zone, *Chem. Eng. Process.*, 2003, vol. 42, pp. 841–846.
8. Trifkovic, M., Sheikhzadeh, M., and Rohani, S., Determination of metastable zone width for combined anti-solvent/cooling crystallization, *J. Cryst. Growth*, 2009, vol. 311, pp. 3640-3650.
9. Kubota, N.A., Unified interpretation of metastable zone widths and induction times measured for seeded solutions, *J. Cryst. Growth*, 2010, vol. 312, pp. 548–554.
10. Sullivan, B.O., The application of in situ analysis to crystallization process development, *PhD Thesis*, Dublin: Univ. College Dublin, 2005.
11. Myerson, A.S. and Jang, S.M., The effect of calcaneal osteotomy on contact characteristics of the tibiotalar joint, *Foot*, 1995, vol. 5, pp. 137–142.
12. Gurbuz, H. and Ozdemir, B., Experimental determination of the metastable zone width of borax decahydrate by ultrasonic velocity measurement, *J. Cryst. Growth*, 2003, vol. 252, pp. 343–349.
13. Barrett, P. and Glennon, B., Characterizing the metastable zone width and solubility curve using Lasentec FBRM and PVM, *Trans. IChemE, Part A: Eng. Res. Des.*, 2002, vol. 80, pp. 799–805.
14. Kubota, N., Effect of sample volume on metastable zone width and induction time, *J. Cryst. Growth*, 2012, vol. 345, pp. 27–33.
15. Azimi, G. and Papangelakis, V.G., *The solubility of gypsum and anhydrite in simulated laterite pressure acid leach solutions up to 250*, *Hydrometallurgy*, 2010, vol. 102, pp. 1–13.
16. Marliacy, P., Solimando, R., Bouroukba, M., and Schuffenecker, L., Thermodynamics of crystallization of sodium sulfate decahydrate in H_2O–NaCl–Na_2SO_4: Application to $Na_2SO_4 \cdot 10H_2O$-based latent heat storage materials, *Thermochim. Acta*, 2000, vol. 344, pp. 85–94.

17. Rodriguez-Navarro, C., Doehne, E., and Sebastian, E., How does sodium sulfate crystallize? Implications for the decay and testing of building materials, *Cem. Concr. Res.*, 2000, vol. 30, pp. 1527–1534.

18. Steiger, M. and Asmussen, S., Crystallization of sodium sulfate phases in porous materials: The phase diagram Na_2SO_4–H_2O and the generation of stress. *Geochim. Cosmochim. Acta*, 2008, vol. 72, pp. 4291–4306.

19. Genkinger, S. and Putnis, A., Crystallization of sodium sulfate: Supersaturation and metastable phases, *Environ. Geol.*, 2007, vol. 52, pp. 329–337.

20. Qiaoli Chen, Jingkang Wang, and Ying Bao, Determination of the crystallization thermodynamics and kinetics of L-tryptophan in alcohols–water system, *Fluid Phase Equilib.*, 2012, vol. 313, pp. 182–189.

21. Heinrich, J. and Ulrich, J., Crystallization kinetics of α-ammonium chloride monitored by in-situ measurement techniques, *Adv. Powder Technol.*, 2011, vol. 22, pp. 190–196.

22. Nyvlt, J., Kinetics of nucleation in solutions, *J. Cryst. Growth*, 1968, vol. 3, pp. 377–383.

23. Chen Xia and Li Hong, Effects of ultrasound on crystal nucleation of Na_2SO_4, *J. Tianjin Univ.*, 2011, vol. 44, pp. 835–839.

24. Nielsen, A.E. and Söhnel, O., Interfacial tensions electrolyte crystal-aqueous solution, from nucleation data, *J. Cryst. Growth*, 1971, vol. 11, pp. 233–242.